Nonlinear Dynamics of Bose-Einstein Condensates with Long-Range Interactions

G. Wunner, H. Cartarius, T. Fabčič, P. Köberle, J. Main and T. Schwidder

Institut für Theoretische Physik 1, Universität Stuttgart, 70550 Stuttgart, Germany

Abstract. The motto of this paper is: Let's face Bose-Einstein condensation through nonlinear dynamics. We do this by choosing variational forms of the condensate wave functions (of given symmetry classes), which convert the Bose-Einstein condensates via the time-dependent Gross-Pitaevskii equation into Hamiltonian systems that can be studied using the methods of nonlinear dynamics. We consider in particular cold quantum gases where long-range interactions between the neutral atoms are present, in addition to the conventional short-range contact interaction, viz. gravity-like interactions, and dipole-dipole interactions. The results obtained serve as a useful guide in the search for nonlinear dynamics effects in numerically exact quantum calculations for Bose-Einstein condensates. A main result is the prediction of the existence of stable islands as well as chaotic regions for excited states of dipolar condensates, which could be checked experimentally.

Keywords: Bose-Einstein condensation, Gross-Pitaevskii equation, nonlinear dynamics effects
PACS: 03.75.Kk, 34.20.Cf, 02.30.-f, 47.20.Ky

1. INTRODUCTION

At sufficiently low temperatures a condensate of weakly interacting bosons can be represented by a single wave function whose dynamics obeys the Gross-Pitaevskii equation [1, 2]. The Gross-Pitaevskii equation can be thought of as the Hartree equation for the ground state of N interacting identical bosons, all occupying the same single-particle orbital ψ. Because of its nonlinearity the equation exhibits features not familiar from ordinary Schrödinger equations of quantum mechanics. For example, Huepe et al. [3, 4] demonstrated that for Bose-Einstein condensates with attractive contact interaction, described by a negative s-wave scattering length, *bifurcations* of the stationary solutions of the Gross-Pitaevskii equation appear, and determined both the stable (elliptic) and the unstable (hyperbolic) branches of the solutions. The bifurcation points correspond to critical particle numbers, above which, for given strength of the attractive interaction, collapse of the condensate sets in. In Bose-Einstein condensates of ^{7}Li [5, 6] and ^{85}Rb atoms [7, 8] these collapses were experimentally observed.

In those condensates the short-range contact interaction is the only interaction to be considered. In Bose-Einstein condensates of *dipolar* gases [9, 10, 11, 12, 13] also a long-range dipole-dipole interaction is present. Alternatively, following a proposal by O'Dell et al. [14, 15], by using a combination of 6 triads of appropriately tuned laser light condensates can be produced in which an attractive long-range gravity-like $1/r$ interaction is present. These types of condensates offer the opportunity to study degenerate quantum gases with adjustable long-range *and* short-range interactions. While the experimental realization of condensates with gravity-like interaction lies still

CP1076, *Let's Face Chaos Through Nonlinear Dynamics: 7th International Summer School and Conference*
edited M. Robnik and V. Romanovski

in the future, the achievement of Bose-Einstein condensation in a gas of chromium atoms [16], with a large dipole moment, has opened the way to promising experiments on dipolar gases [17], which could show a wealth of novel phenomena [18, 19, 20, 21]. In particular, the experimental observation of the collapse of dipolar quantum gases has been reported [22] which occurs when the contact interaction is reduced, for a given particle number, below some critical value using a Feshbach resonance.

In this experimental situation it is most timely and appropriate to extend the investigations of the nonlinearity effects of the Gross-Pitaevskii equation to quantum gases in which both the contact interaction and a long-range interaction is active, and this is the topic of the present paper.

2. SCALING PROPERTIES OF THE GROSS-PITAEVSKII EQUATIONS WITH LONG-RANGE INTERACTIONS

2.1. Gravity-like interaction, isotropic trap

For an additional gravity-like long-range interaction $V_u(\vec{r},\vec{r}') = -u/|\vec{r}-\vec{r}'|$ the time-dependent Gross-Pitaevskii equation for the orbital ψ reads

$$\left[-\Delta+\gamma^2 r^2+N8\pi\frac{a}{a_u}|\psi(\vec{r},t)|^2-2N\int\frac{|\psi(\vec{r}',t)|^2}{|\vec{r}-\vec{r}'|}d^3\vec{r}'\right]\psi(\vec{r},t)=i\frac{\partial}{\partial t}\psi(\vec{r},t)\,, \qquad (1)$$

where we have used [23] the "Bohr radius" $a_u = \hbar^2/(mu)$, the "Rydberg energy" $E_u = \hbar^2/(2ma_u^2)$, and the Rydberg time $\hbar/E_u$ as natural units of length, energy, and time, respectively, to bring the equation in dimensionless form. Furthermore, in (1) a is the s-wave scattering length, which characterizes the strength of the contact interaction $V_s = \delta(\vec{r}-\vec{r}')4\pi a\hbar^2/m$, N is the particle number, and $\gamma = \hbar\omega_0/(2E_u)$ is the dimensionless trap frequency. It can be shown [23] that the solutions of (1) do not depend on all these three physical quantities but only on the two relevant parameters γ/N^2 and N^2a/a_u. Thus one has, e.g., for the mean-field energy $E(N,N^2a^*/a_u,\gamma/N^2)/N^3 = E(N=1,a/a_u,\gamma)$, with $N^2a^*/a_u = a/a_u$.

2.2. Dipolar interaction, axisymmetric trap

In Bose condensates of ^{52}Cr atoms [16], which possess a large magnetic moment of $\mu = 6\mu_B$, the long-range dipole-dipole interaction

$$V_{dd}(\vec{r},\vec{r}') = \frac{\mu_0\mu^2}{4\pi}\frac{1-3\cos^2\theta'}{|\vec{r}-\vec{r}'|^3} \qquad (2)$$

must also be considered. Defining the dipole length by $a_d = \mu_0\mu^2 m/(2\pi\hbar^2)$, and using as unit of energy $E_d = \hbar^2/(2ma_d^2)$, of frequency $\omega_d = 2E_d/\hbar$ and of time $\hbar/E_d$, one obtains the Gross-Pitaevskii equation for dipolar gases in axisymmetric traps in dimensionless

form

$$\left[-\Delta+\gamma_\rho^2\rho^2+\gamma_z^2 z^2+N8\pi\frac{a}{a_\mathrm{d}}|\psi(\vec{r},t)|^2 + N\int|\psi(\vec{r}\,',t)|^2\frac{(1-3\cos^2\vartheta')}{|\vec{r}-\vec{r}\,'|^3}d^3\vec{r}\,'\right]\psi(\vec{r},t) = i\frac{\partial}{\partial t}\psi(\vec{r},t)\,. \tag{3}$$

The physical parameters characterizing the condensates are the particle number N, the scattering length a/a_d and the trap frequencies γ_ρ and γ_z perpendicular to and along the direction of alignment of the dipoles (alternatively, the geometric mean ($\bar{\gamma}=\gamma_\rho^{2/3}\gamma_z^{1/3}$ and the aspect ratio $\lambda=\gamma_z/\gamma_\rho$ is used). However, a closer inspection of the scaling properties of (3) reveals [24] that the solutions depend only on three parameters, viz. $N^2\bar{\gamma}$, λ, a/a_d. For the mean-field energy, e.g., the scaling law reads $E(N,a/a_\mathrm{d},N^2\bar{\gamma}^*,\lambda) = E(N=1,a/a_\mathrm{d},\bar{\gamma},\lambda)/N$, with $N^2\bar{\gamma}^*=\bar{\gamma}$.

3. QUANTUM RESULTS: SOLUTIONS OF THE STATIONARY GROSS-PITAEVSKII EQUATIONS

For the $1/r$ interaction (monopolar quantum gases) we have solved [23] the stationary Gross-Pitaevskii equation both variationally, using an isotropic Gaussian-type orbital $\psi=A\exp(-k^2r^2/2)$, and numerically accurate, by outward integration of the nonlinear Schrödinger equation. For the dipole-dipole interaction (dipolar quantum gases) we have performed a variational calculation [24] using an axisymmetric Gaussian-type orbital $\psi=A\exp(-k_\rho^2\rho^2/2-k_z^2z^2/2)$.

Fig. 1 shows the results for the chemical potential (eigenvalue of the stationary Gross-Pitaevskii equation) for the two interactions, plotted as a function of the scattering length. As can be seen, below a critical scattering length no stationary solutions exist, while two stationary solutions are born at the critical scattering length in a tangent bifurcation. At the bifurcation point the chemical potential, the mean-field energy, and the wave functions of the two branches of solution are identical. Such behavior is obviously a consequence of the nonlinearity of the underlying Schrödinger equation, and is reminiscent of exceptional points [25, 26] discussed so far only in the context of open quantum systems with non-Hermitian Hamiltonians (see Ref. [27] for references). In fact, a closer inspection shows [27] that the bifurcation points can be identified as exceptional points: traversing circles around them in the complex-extended parameter plane, the eigenvalues are permuted, which is a clear signature of exceptional points.

4. NONLINEAR DYNAMICS OF BOSE-EINSTEIN CONDENSATES WITH ATOMIC LONG-RANGE INTERACTIONS

Starting point of accurate numerical calculations are the time-dependent Gross-Pitaevskii equations (1) and (3). For variational calculations one makes use of the fact that these equations follow from the variational principle $||i\dot{\phi}(t)-H\psi(t)||^2 = \min$,

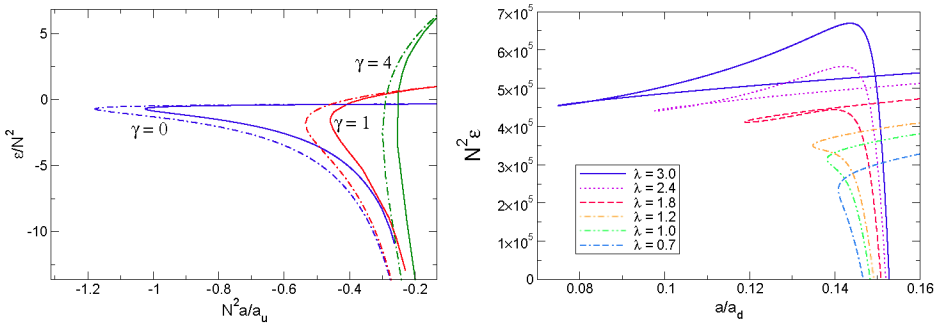

FIGURE 1. Bifurcations of the particle-number scaled chemical potential. Left: $1/r$ interaction, for different trap frequencies γ (in units of N^2); solid curves: accurate numerical calculation, dashed curves: variational calculation. Right: dipole-dipole interaction, variational results for the geometric mean trap frequency $N^2\bar{\gamma} = 3.4 \times 10^4$ used in the experiments of Koch et al. [22] and different values of the trap aspect ratio λ.

where the variation is performed with respect to ϕ, and finally ϕ is set equal to ψ. Using a complex parametrization of the trial wave function $\psi(t) = \chi(\vec{\lambda}(t))$, the variation leads to equations of motion for the parameters $\vec{\lambda}$ (cf. [28])

$$\left\langle \frac{\partial\psi}{\partial\vec{\lambda}} \middle| i\dot{\psi} - H\psi \right\rangle = 0 \leftrightarrow K\dot{\vec{\lambda}} = -i\vec{h} \text{ with } K = \left\langle \frac{\partial\psi}{\partial\vec{\lambda}} \middle| \frac{\partial\psi}{\partial\vec{\lambda}} \right\rangle, \vec{h} = \left\langle \frac{\partial\psi}{\partial\vec{\lambda}} \middle| H \middle| \psi \right\rangle. \qquad (4)$$

4.1. Time evolution of condensates with $1/r$ interaction, variational and exact

For simplicity we consider the case of selftrapping, with no external trap. As one can convince oneself, the results can be easily generalized to the case where an external radially symmetric trap potential is present. We choose a Gaussian trial wave function $\psi(r,t) = \exp\{i[A(t)r^2 + \gamma(t)]\}$, where A and γ are complex functions of time, whose equations of motion follow from (4). Decomposing A into real and imaginary parts, $A = A_r + iA_i$, and replacing them by two other dynamical quantities [29, 30], $q = \sqrt{3/(4A_i)} \equiv \sqrt{\langle r^2 \rangle}$, $p = A_r\sqrt{3/A_i}$, converts those equations into the canonical equations of motion for p and q that follow from the Hamiltonian

$$E = H(q,p) = T + V = p^2 + \frac{9}{4q^2} + \frac{3\sqrt{3}a}{2\sqrt{\pi}q^3} - \frac{\sqrt{3}}{\sqrt{\pi}q}. \qquad (5)$$

In this way the Gross-Pitaevskii equation is mapped onto the Hamiltonian of a one-dimensional classical autonomous system with a nonlinear potential $V(q)$. The potential has no extremum for $a < a_{\rm cr} = -3\pi/8 \approx -1.18$, possesses a saddle point for $a = a_{\rm cr}$, and a maximum and a minimum for $a > a_{\rm cr}$. The critical scattering length corresponds to the bifurcation point in the variational calculation. For different values of a (in units

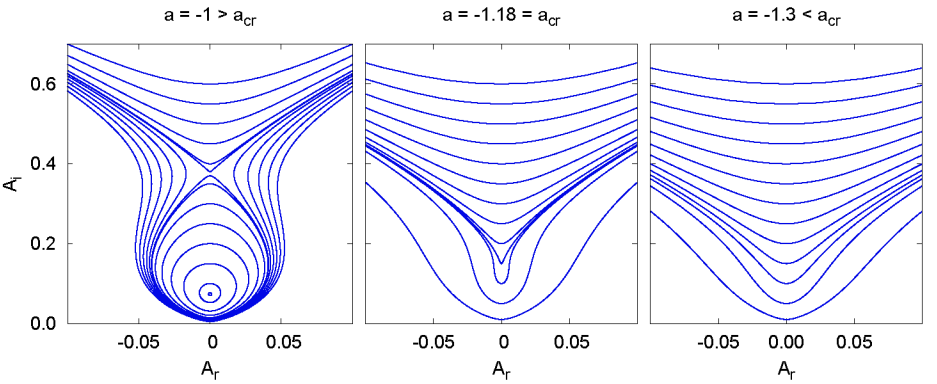

FIGURE 2. Phase portraits of the dynamics of the complex width function $A(t)$ associated with the Hamiltonian (5) for attractive $1/r$ interaction for different values of the scattering length a, measured in units of a_u. Left: $a = -1 > a_{\rm cr}$: two stationary states appear as fixed points; middle: $a = -1.18 = a_{\rm cr}$: coalescence of the fixed points; right: $a = -1.3 < a_{\rm cr}$: no stationary solutions exist.

of a_u) phase portraits of trajectories moving according to the Hamiltonian (5) are shown in Fig. 2.

The linear stability analysis of both the variational and the exact quantum stationary solutions proves [30] that the state corresponding to the elliptical fixed-point indeed is dynamically stable (small perturbations of the state show oscillating behavior), while the stationary state corresponding to the hyperbolic fixed-point is dynamically unstable (exponential growth of small perturbations).

This behavior is recovered in exact numerical solutions of the time-dependent Gross-Pitaevskii equation with $1/r$ interaction, but also new features emerge. The solution is carried out [30] using the split-operator technique and fast Fourier transforms. To investigate the behavior of condensate wave functions in the vicinity of the exact numerical stable and unstable stationary states, we consider condensates which are obtained by deforming the stationary states by $\psi(r) = f \cdot \psi_{\pm}(r \cdot f^{2/3})$, where f is a numerical stretching factor (this choice of the perturbation does not affect the norm of the state).

In Fig. 3 we show examples of the exact BEC dynamics in the vicinity of the unstable and stable stationary states. In Fig. 3 a) we start the time evolution with the numerical solution for the unstable stationary state (in the classical picture this corresponds to the trajectory starting at the hyperbolic fixed point, see left part of Fig. 2). Because of unavoidable numerical deviations from the theoretically exact unstable state, the wave function determined numerically is stationary only for some time but then begins to oscillate. Obviously we have started with a state which in the variational picture would be located in the elliptical domain close to the hyperbolic fixed point. Note, however, that the oscillation is not strictly periodic. By contrast, in Fig. 3 b), where the time evolution starts with the unstable stationary state stretched by a factor of $f = 1.001$, as time proceeds the wave function contracts towards the origin, and the condensate collapses. In the variational picture this corresponds to a trajectory initially close to the hyperbolic fixed point but located on the hyperbolic side. Note that in a realistic

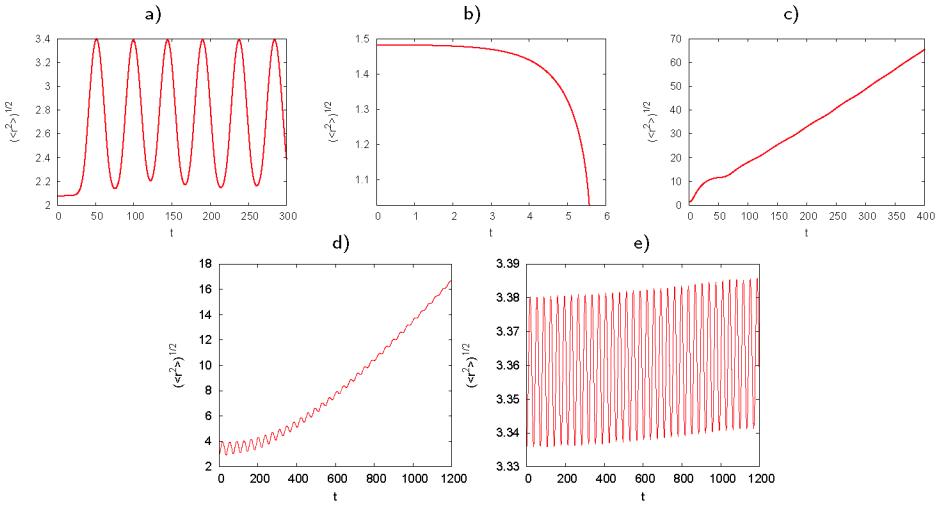

FIGURE 3. Time evolution, for attractive $1/r$ interaction, of the root-mean-square widths of the condensate wave functions in the vicinity of the unstable (panels a), b), c)) and the stable stationary (panels d), e)) state. a): Scaled scattering length (in units of a_d) a = -1.0, stretching factor f= 1.00; b): a = -0.85, f = -1.001; c): a = -0.85, f = 0.99; d): a = -0.85, f =1.25, and e): a = -0.85, f = 1.01.

experimental situtation during the collapse further mechanisms have to be taken into account, such as inelastic collisions. The inclusion of such mechanisms, however, clearly goes beyond the scope of the present paper.

Figure 3 c) displays a behavior not present in the variational analysis. We start again in the vicinity of the unstable stationary state ($f = 0.99$) and find that the width of the condensate gradually grows and grows. An inspection of the wave function on a logarithmic scale shows [30] that wave function amplitude builds up at large distances from the origin, giving rise to this behavior. Finally, Fig. 3 d), e) show examples for the quantum mechanical time evolution of condensates in the vicinity of the stable ground state. For a large stretching factor (panel d)) the condensate is found to oscillate and to expand, while for a small stretching factor (panel e)) we find the quasiperiodic oscillations that we would expect from the variational analysis. This demonstrates that the variational nonlinear dynamics approach is capable of predicting essential features of the exact quantum mechanical time behavior of the condensates, but that the quantum mechanical behavior is even richer.

4.2. Dynamics of condensates with dipolar interaction, variational

We choose a Gaussian trial wave function adapted to the axisymmetric trap geometry, $\psi(\rho,z,t) = e^{i(A_\rho \rho^2 + A_z z^2 + \gamma)}$, where the complex width parameters A_ρ, A_z, and the complex phase are functions of time. Their dynamical equations follow from the time-

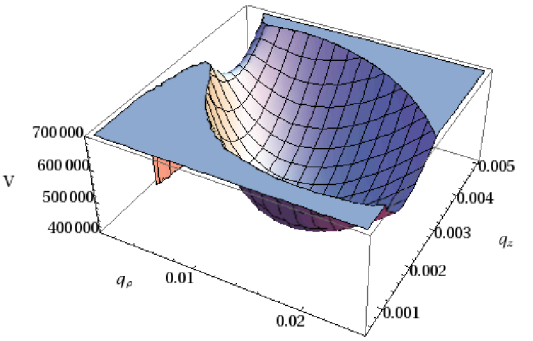

FIGURE 4. Potential $V(q_\rho, q_z)$ in the Hamiltonian (7) for dipole-dipole long-range interaction.

dependent variational principle (4). Introducing new variables q_ρ, q_z, p_ρ, p_z via

$$\mathrm{Re}\, A_\rho = p_\rho/(4q_\rho), \;\; \mathrm{Im}\, A_\rho = 1/(4q_\rho^2), \;\; \mathrm{Re}\, A_z = p_z/(4q_z), \;\; \mathrm{Im}\, A_z = 1/(8q_z^2) \qquad (6)$$

one finds that their dynamical equations are equivalent to the canonical equations of motion belonging to the Hamiltonian

$$\begin{aligned} H &= T+V = \frac{p_\rho^2}{2} + \frac{p_z^2}{2} + \frac{1}{2q_\rho^2} + 2\gamma_\rho^2 q_\rho^2 + \frac{a/a_\mathrm{d}}{2\sqrt{2\pi}q_\rho^2 q_z} + \frac{1}{8q_z^2} + 2\gamma_z^2 q_z^2 \\ &+ \frac{1+q_\rho^2/q_z^2 - 3q_\rho^2 \arctan\sqrt{q_\rho^2/(2q_z^2)-1}\Big/\left(q_z^2\sqrt{2q_\rho^2/q_z^2-4}\right)}{6\sqrt{2\pi}q_\rho^4 q_z\left(1/q_z^2 - 2/q_\rho^2\right)}. \end{aligned} \qquad (7)$$

Thus the variational ansatz has turned the problem into one corresponding to a two-dimensional nonintegrable Hamiltonian system, which will exhibit all the features familiar from nonlinear dynamics studies of such systems. From the shape of the potential, which is shown in Fig. 4 as a function of the "position" variables q_ρ, q_z, these features can already be read off qualitatively. At the potential minimum sits the stable stationary ground state (elliptic fixed point), while at the saddle point one finds an unstable excited stationary state (hyperbolic fixed point). To quantitatively characterize the dynamics of the variational condensate wave functions we follow the trajectories in the four-dimensional configuration space spanned by the coordinates of the real and imaginary parts of A_ρ and A_z. Since the total mean-field energy is a constant of motion the trajectories are confined to three-dimensional hyperplanes, and their behavior can most conveniently be visualized by two-dimensional Poincaré surfaces of section defined by requiring one of the coordinates to assume a fixed value.

We consider Poincaré surfaces of section defined by the condition that the imaginary part of $A_z(t)$ is zero. Each time the trajectory crosses the plane $\mathrm{Im}\, A_z = 0$, the real and imaginary parts of $A_\rho(t) = A_\rho^r(t) + iA_\rho^i(t)$ are recorded. In Fig. 5 surfaces of section are plotted for five different, increasing, values of the mean-field energy. The physical parameters of the experiment of Koch et al. [22] are adopted, and the scattering length

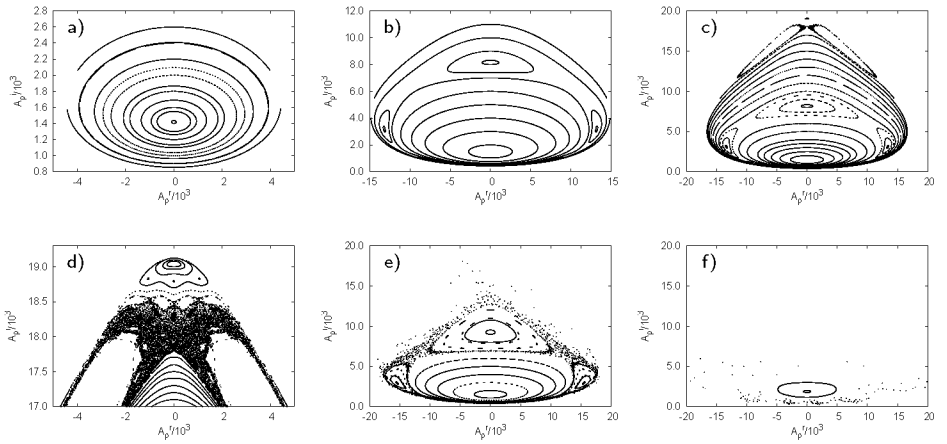

FIGURE 5. Poincaré surfaces of section of the condensate wave functions for dipolar interaction represented by their width parameters at the scaled trap frequency $N^2\tilde{\gamma} = 3.4 \times 10^4$, aspect ratio $\lambda = 6$, and the scattering length $a/a_{\rm d} = 0.1$. The surfaces of section correspond to increasing values of the mean-field energy (in units of $E_{\rm d}$): a) $NE = 4.5 \times 10^5$, b) $NE = 6.00 \times 10^5$, c) and d) $NE = 6.24 \times 10^5$, e) $NE = 9 \times 10^5$, f) $NE = 6.00 \times 10^6$.

is fixed to $a/a_{\rm d} = 0.1$, away from its critical value. At these parameters, the variational mean-field energy of the ground state is $NE_{\rm gs} = 4.24 \times 10^5$ (in units of $E_{\rm d}$) and represents the local minimum on the two-dimensional mean-field energy landscape, plotted as a function of the width parameters. The variational energy of the second, unstable, stationary state at these experimental parameters is $NE_{\rm es} = 6.24 \times 10^5$, it corresponds to the saddle point on the mean-field energy surface. Between these two energy values the motion on the trajectories is bound, while for energies above the saddle-point energy the motion on the trajectories can become unbound: once the saddle point is traversed by a trajectory $A_\rho(t)$, $A_z(t)$, the parameters run to infinity, meaning a shrinking of the quantum state to vanishing width, i e., a collapse of the condensate takes place.

The energy in Fig. 5 a) lies slightly above the energy of the stationary ground state. The initially stationary state has evolved into a periodic orbit (fixed point in the surface of section), corresponding to a state of the condensate whose motion is periodic. The oscillations of the width parameters $A_\rho(t)$ and $A_z(t)$ represent oscillatory stretchings of the condensate along the ρ and z directions. The stable *periodic* orbit in the surface of section is surrounded by elliptical, quasi-periodic orbits, representing quasi-periodic oscillations of the condensate. As the energy is increased further, in Fig. 5 b), new periodic and quasi-periodic orbits are born, and the motion is still regular. In Fig. 5 c) we have reached the saddle-point energy. Now chaotic orbits have appeared in the vicinity of the unstable excited stationary state (hyperbolic fixed point). Figure 5 d) shows an enlargement of this region in phase space. In contrast to the (quasi-) periodic stretching oscillations of the condensate within the elliptical islands, the chaotic motion of the parameters describes a condensate which does not yet collapse but whose widths fluctuate irregularly.

In the surfaces of section shown in Fig. 5 e) and f), with mean-field energies well above the saddle-point energy, regular islands are still clearly visible. These stable islands are surrounded by chaotic trajectories. Since ergodic motion along these trajectories comes close to every point in the configuration space, the chaotic motion sooner or later leads to a crossing of the saddle point and then to the collapse of the condensate wave functions. It can be seen that with growing energy above the saddle point the sizes of the stable regions shrink. The kinematically allowed regions surrounding the stable islands are hardly recognizable any more since high above the saddle-point energy the chaotic motion becomes more and more unbound, and thus trajectories cross the Poincaré surfaces of section only a few times, if ever, before they escape to infinity and collapse takes place.

It must be stressed, however, that stable islands persist even far above the saddle-point energy, implying the existence of quasi-periodically oscillating nondecaying modes of dipolar condensate wave functions.

5. SUMMARY AND CONCLUSIONS

We have demonstrated that variational forms of the Bose-Einstein condensate wave functions convert the condensates via the Gross-Pitaevskii equation into Hamiltonian systems that can be studied using the methods of nonlinear dynamics. We have also shown that these results serve as a useful guide in the search for nonlinear dynamics effects in the numerically accurate quantum calculations of Bose-Einstein condensates with long-range interactions. The existence of stable islands as well as chaotic regions for excited states of dipolar Bose-Einstein condensates is a result that could be checked experimentally. One way of creating the collectively excited states one might think of is to prepare the condensate in the ground state, and then to non-adiabatically reduce the trap frequencies.

One might question whether the Gross-Pitaevskii equation is adequate to describe the types of complex dynamics discussed in this paper in "real" condensates. For example, in the chaotic regime local density maxima might occur for which losses by two-body or three-body collisions would have to be taken into account. However, by virtue of the scaling laws discussed in Sections 2.1 and 2.2 parameter ranges can always be found where the particle densities remain small even in these regimes, and the Gross-Pitaevskii equation is applicable.

The advantage of the simple variational ansatz adopted in this paper is that the analysis of the nonlinear dynamical properties of Bose-Einstein condensates becomes particularly transparent. Numerical quantum calculations to confirm the variational findings for dipolar gases and the extensions to structured condensate states [31, 32] are under way. We have already seen in Sec. 4.1, by comparing variational and accurate numerical quantum results for Bose-Einstein condensates with attractive $1/r$ interaction, that the nonlinear dynamical properties predicted by the variational calculation were confirmed by the full quantum calculations. We therefore have good reason to believe that this will also be true once the full quantum calculations of the dynamics of excited condensate wave functions of dipolar gases have become available.

ACKNOWLEDGMENTS

Part of this work has been supported by Deutsche Forschungsgemeinschaft. H.C. is grateful for support from the Landesgraduiertenförderung of the Land Baden-Württemberg.

REFERENCES

1. E. P. Gross, *Nuovo Cimento* **20**, 454 (1961).
2. L. P. Pitaevskii, *Sov. Phys. JETP* **13**, 451 (1961).
3. C. Huepe, S. Métens, G. Dewel, P. Borckmans, and M. E. Brachet, *Phys. Rev. Lett.* **82**, 1616–1619 (1999).
4. C. Huepe, L. S. Tuckerman, S. Métens, and M. E. Brachet, *Phys. Rev. A* **68**, 023609 (2003).
5. C. A. Sacket, J. M. Gerton, M. Welling, and R. G. Hulet, *Phys. Rev. Lett.* **82**, 876 (1999).
6. J. M. Gerton, D. Strekalov, I. Prodan, and R. G. Hulet, *Nature* **406**, 692 (2000).
7. E. A. Donley, N. R. Claussen, S. L. Cornish, , J. L. Roberts, E. A.Cornell, and C. E. Wiemann, *Nature* **412**, 295 (2001).
8. J. L. Roberts, N. R. Claussen, S. L. Cornish, E. A. Donley, E. A. Cornell, and C. E. Wieman, *Phys. Rev. Lett.* **86**, 4211 (2001).
9. L. Santos, G. V. Shlyapnikov, P. Zoller, and M. Lewenstein, *Phys. Rev. Lett.* **85**, 1791 (2000).
10. M. Baranov, L. Dobrek, K. Góral, L. Santos, and M. Lewenstein, *Phys. Scr.* **T102**, 74 (2002).
11. K. Góral, L. Santos, and M. Lewenstein, *Phys. Rev. Lett.* **88**, 170406 (2002).
12. K. Góral, and L. Santos, *Phys. Rev. A* **66**, 023613 (2002).
13. S. Giovanazzi, A. Görlitz, and T. Pfau, *J. Opt. B.* **5**, S208 (2003).
14. D. O'Dell, S. Giovanazzi, G. Kurizki, and V. M. Akulin, *Phys. Rev. Lett.* **84**, 5687 (2000).
15. S. Giovanazzi, D. O'Dell, and G. Kurizki, *Phys. Rev. A* **63**, 031603(R) (2001).
16. A. Griesmaier, J. Werner, S. Hensler, J. Stuhler, and T. Pfau, *Phys. Rev. Lett.* **94**, 160401 (2005).
17. J. Stuhler, A. Griesmaier, T. Koch, M. Fattori, T. Pfau, S. Giovanazzi, P. Pedri, and L. Santos, *Phys. Rev. Lett.* **95**, 150406 (2005).
18. S. Giovanazzi, A. Görlitz, and T. Pfau, *Phys. Rev. Lett.* **89**, 130401 (2002).
19. L. Santos, G. V. Shlyapnikov, and M. Lewenstein, *Phys. Rev. Lett.* **90**, 250403 (2003).
20. S. Yi, L. You, and H. Pu, *Phys. Rev. Lett.* **93**, 040403 (2004).
21. D. H. J. O'Dell, S. Giovanazzi, and C. Eberlein, *Phys. Rev. Lett.* **92**, 250401 (2004).
22. T. Koch, T. Lahaye, J. Metz, B. Fröhlich, A. Griesmaier, and T. Pfau, *Nature Physics* **4**, 218–222 (2008).
23. I. Papadopoulos, P. Wagner, G. Wunner, and J. Main, *Phys. Rev. A* **76** (2007).
24. P. Köberle, H. Cartarius, T. Fabčič, J. Main, and G. Wunner, *New J. Phys.* (2008), submitted, Preprint: arXiv:0802.4055v2.
25. W. D. Heiss, *Eur. Phys. J. D* **7**, 1–4 (1999).
26. T. Kato, *Perturbation theory for linear operators*, Springer, Berlin, 1966.
27. H. Cartarius, J. Main, and G. Wunner, *Phys. Rev. A* **77**, 013618 (2008).
28. T. Fabčič, J. Main, and G. Wunner, *Nonlinear Phenomena in Complex Systems* **10**, 86–91 (2007).
29. J. Broeckhove, L. Lathouwers, and P. V. Leuven, *J. Phys. A* **22**, 4395–4408 (1989).
30. H. Cartarius, T. Fabčič, J. Main, and G. Wunner, *Phys. Rev. A* **78**, 013615 (2008).
31. K. Góral, K. Rzążewski, and T. Pfau, *Phys. Rev. A* **61**, 051601(R) (2000).
32. O. Dutta, and P. Meystre, *Phys. Rev. A* **75**, 053604 (2007).